Influence of structural complexity of the Rumperöd forest on evapotranspiration

Madeleine Durdek

Madeleine Durdek (2023).
Influence of structural complexity of the Rumperöd forest on evapotranspiration
Bachelor degree thesis, 15 credits in Physical Geography and Ecosystem Analysis
Department of Physical Geography and Ecosystem Science, Lund University

Level: Bachelor of Science (BSc)

Course duration: *March* 2023 until *June* 2023

Disclaimer

This document describes work undertaken as part of a program of study at the University of Lund. All views and opinions expressed herein remain the sole responsibility of the author, and do not necessarily represent those of the institute.

Cover image: *Mixed Forest. Shmetsk Near Narva*. Oil painting by Ivan Shishkin (1888)

Influence of structural complexity of the Rumperöd forest on evapotranspiration

Madeleine Durdek

Bachelor thesis, 15 credits, in Physical Geography and Ecosystem Analysis

Supervisor 1 Patrik Vestin
Department of Physical Geography and Ecosystem Science

Supervisor 2 Tobias Biermann
Centre for Environmental and Climate Science

Exam committee:
Cecilia Akselsson
Ulrik Mårtensson

Department of Physical Geography and Ecosystem Science

Abstract

The influence of Forest Structural Complexity (FSC) on evapotranspiration (ET) was investigated in a mixed forest of Southern Sweden where micrometeorological Eddy Covariance (EC) measurements were conducted for the years 2015 to 2022. For each year, the top 25% of Vapour Pressure Deficit (VPD) were selected to emphasize the response of ET to the driest atmospheric conditions. FSC was quantified using three indices. First, the Gini index represents the variation in basal area. Second, the Rumperöd Index (RI), specifically created for this study, considers the difference in tree height weighed by basal area, and includes stand density. The third index, named β, quantifies the proportion of coniferous species. These indices were calculated for eight transects around the EC tower. To investigate the influence of FSC on ET, fluxes were sorted by wind direction and compared to the indices per transect. To verify that the residuals of ET to VPD were dependent on the transects, a generalised linear model using a Wald Chi-Square test was performed.

Species composition had a great influence on ET under increasing dry conditions: coniferous transects usually kept photosynthesizing at a higher VPD than deciduous. Species composition associated with high variation in basal area (Gini index) could explain higher annual ET. The ET response to a high complexity in RI resembled that of the Gini index, but high stand density and poor species diversity enhanced competition for water resources, hence a lower annual ET. The FSC indices together explain patterns of ET and show its dependence on FSC, which is supported by the statistical tests. This study shows the importance of structural complexity to sustain hydraulic functioning of forest stands under dry conditions.

Keywords: Forest structural complexity; evapotranspiration; vapour pressure deficit; eddy covariance.

List of abbreviations:

BA: Basal Area
CCF: Continuous Cover Forestry
DBH: Diameter at Breast Height
ET: Evapotranspiration
FSC: Forest Structural Complexity
GLM: Generalised Linear Model
RI: Rumperöd Index
VPD: Vapour Pressure Deficit

Table of Contents

1 Introduction

Since the late 19th century, forests of Fennoscandia, that is Scandinavia, Finland and the Russian regions of Kola and Karelia (Seppälä, 2005), have been increasingly managed with a technique called rotation forestry (Lundmark et al., 2013). This practice creates a strong competition for light between trees to accelerate growth, increase the frequency of cuttings and maximise profitability. Typical rotation forests consist of rows of even-aged trees, usually the same species. This type of forest management is being increasingly criticised. The generated poor structural complexity is a barrier to biodiversity, and single-species stands are more vulnerable to invasive pests as well as pathogens (Macpherson et al., 2017; Spiecker, 2003). Besides, rotation forestry involves clearcuts, well-known for inducing nutrient leakage (Gundersen et al., 2011; Saarsalmi et al., 2010; Vitousek et al., 1979) and releasing greenhouse gases (Vestin, 2017; Vestin et al., 2020, 2022).

In light of these drawbacks and climate change, alternative practices such as Continuous Cover Forestry (CCF) are reintroduced. CCF encourages selective cutting instead of clear cutting, and mimics natural disturbances of untouched ecosystems, thereby contributing to forest structural complexity (FSC) (Ekholm et al., 2023). McElhinny et al. (2005) define FSC as "the measure of the number of different attributes present and the relative abundance of each of these attributes" in a forest stand. Examples of such attributes are tree height, tree diameter, basal area, species composition, spacing in-between trees or canopy cover. Recent studies (Bachofen et al., 2023; Leonard et al., 2022) have shown that FSC has a beneficial influence on biosphere-atmosphere water exchanges, which makes CCF a key component in forest resilience to climate change and the increased frequency of droughts and heat waves induced (Bednar-Friedl et al., 2022).

FSC influences evapotranspiration (ET) (Leonard et al., 2022) and transpiration sensitivity to Vapour Pressure Deficit (VPD) (Bachofen et al., 2023). ET is the combination of evaporation and transpiration, i.e., the sum of water vapour emitted from the biosphere as latent heat (Chapin et al., 2011b). VPD is the difference between the actual air water vapour pressure and saturation vapour pressure (Grossiord et al., 2020). It is a measure of how dry the air is and how much more water it can still hold. As warm air can contain more water (Ahrens & Henson, 2018), a rise in VPD draws out moisture from the surface, thereby increasing ET. This vertical movement of water from the surface to the atmosphere makes VPD a dynamic and useful measure of drought (Gamelin et al., 2022). Hydraulic stress induced by persistently high VPD leads plants to close their stomata, which impedes gaseous exchanges between the leaves and the atmosphere (Bachofen et al., 2023; Grossiord et al., 2020; Johnson & Ferrell, 2006). Photosynthesis no longer occurs, eventually leading to defoliation and plants death. This phenomenon leads the relationship between transpiration and VPD to be non-linear, transpiration increasing with increasing VPD until it decreases when the stomata close. ET is one of the main components of the water and energy cycle and to include FSC into hydrological and climate models can potentially enhance our understanding of fluxes and improve our predictions of forests' response to droughts.

Modelled estimations of daily ET were improved by 26% by including FSC and associated canopy openness and radiation variability (Leonard et al., 2022). Canopy openness influences how much radiation that can reach the ground, thus how much evaporation occurs. Bachofen et

al. (2023) found that FSC in Central Europe is the main driver of transpiration sensitivity to VPD. More specifically, they found that stand Basal Area (BA), defined as the sum of the cross-sectional area of all trees at breast height per unit area (Bettinger et al., 2017), was "the main driver of maximum tree transpiration and the sensitivity of tree transpiration to VPD". Bachofen et al. (2023) concluded that stands with high BA are less sensitive to transpiration in response to increasing VPD compared to low BA-stands. One discussed explanation is that microclimates within the canopy are created by high BA-stands. Paul-Limoges et al. (2017), who studied below-canopy contributions to ecosystem carbon dioxide fluxes in a mixed forest, argue that leaves in the below-canopy are not as well coupled to the atmosphere as leaves at the top of the canopy. In other words, the water exchange from the leaf to the atmosphere is not as efficient for below-canopy leaves compared to leaves exposed above the canopy. Thus, multi-layered canopies create microclimates that influence transpiration. A multitude of methods exist to quantify FSC (McElhinny et al., 2005), and the amount of factors included or the type of index chosen is, in the end, subjective. Nevertheless, McElhinny et al. (2005) conveyed in a literature review that a reductionist approach could provide a more objective dataset, i.e., a minimum of attributes and a simple mathematical system are preferrable.

The findings of Bachofen et al. (2023) and Leonard et al. (2022) represents valuable information for our understanding of forests' vulnerability to global warming. Bachofen et al. (2023) compared 25 forests across Europe, implying a large difference in climatic and edaphic conditions, which they had to include as separate effects in their study. To analyse the sole effect of FSC on ET, it is relevant to investigate it at a smaller scale and at a single site. The influence of FSC on ET in a mixed coniferous and deciduous forest remains unexplored. If the outcome of such an experiment would show that FSC does have a significant impact on ET at a stand scale, this would demonstrate the importance of mixed coniferous and deciduous stands being structurally diverse.

The aim of this study was to answer the following questions:
- o Does forest structural complexity influence evapotranspiration fluxes at a stand scale?
- o If yes, how does evapotranspiration respond to increasingly dry conditions depending on forest structural complexity?

I hypothesize that a high FSC will influence ET by sustaining water exchange under dry conditions.

2 Material and Methods

2.1 Study site

Forests of Southern Sweden benefit from an oceanic climate –Cfb according to Köppen climate classification (Chen, n.d.), making the region of Scania unique in comparison to the rest of the country where boreal forests are essentially coniferous. Rumperöd is a mixed forest located at 56° 20'00" N 14° 06'45" E. It is privately owned and is situated in Östra Göinge municipality, in Scania County. Sandy moraine is the dominating soil type, and the elevation

ranges between 76 and 107 metres above sea level. The study site spans 40 to 60 hectares (ha) and mainly consists of Norway spruce (*Picea abies*), Scots pine (*Pinus sylvestris*), English oak (*Quercus robur*), European beech (*Fagus sylvatica*), silver birch (*Betula pendula*) and downy birch (*Betula pubescens*) (Westin, 2015). It has been managed using CCF since the 1950s and was never fully clearcut for a long time before that; in this sense, it is a well-preserved, biodiverse stand (Westin, 2015; D. Göransson, personal communication, August 15, 2022). The study site is managed using selective cutting, with the objective to leave a minimum of 100 m³/ha, but preferably more, after each cutting. This long history of selective cutting was one of the reasons for choosing Rumperöd as a study site. It was essential to test the drought in a forest stand free from the influence of clear-cuttings. Furthermore, the increases in mean warming, heat extremes and heavy precipitation already observed in this part of Europe since the 1980s, are expected to keep increasing in the future, according to two different climate scenarios (Bednar-Friedl et al., 2022). The site had been subjected to diverse studies since its establishment; for instance, Delin (2019) studied the site's response to the 2018 drought compared to a Norway spruce stand of the same region. Westin (2015) compared remote sensing techniques and field measurements to quantify above ground biomass of the forest. Figure 1 shows the location of the Rumperöd forest in Southern Sweden.
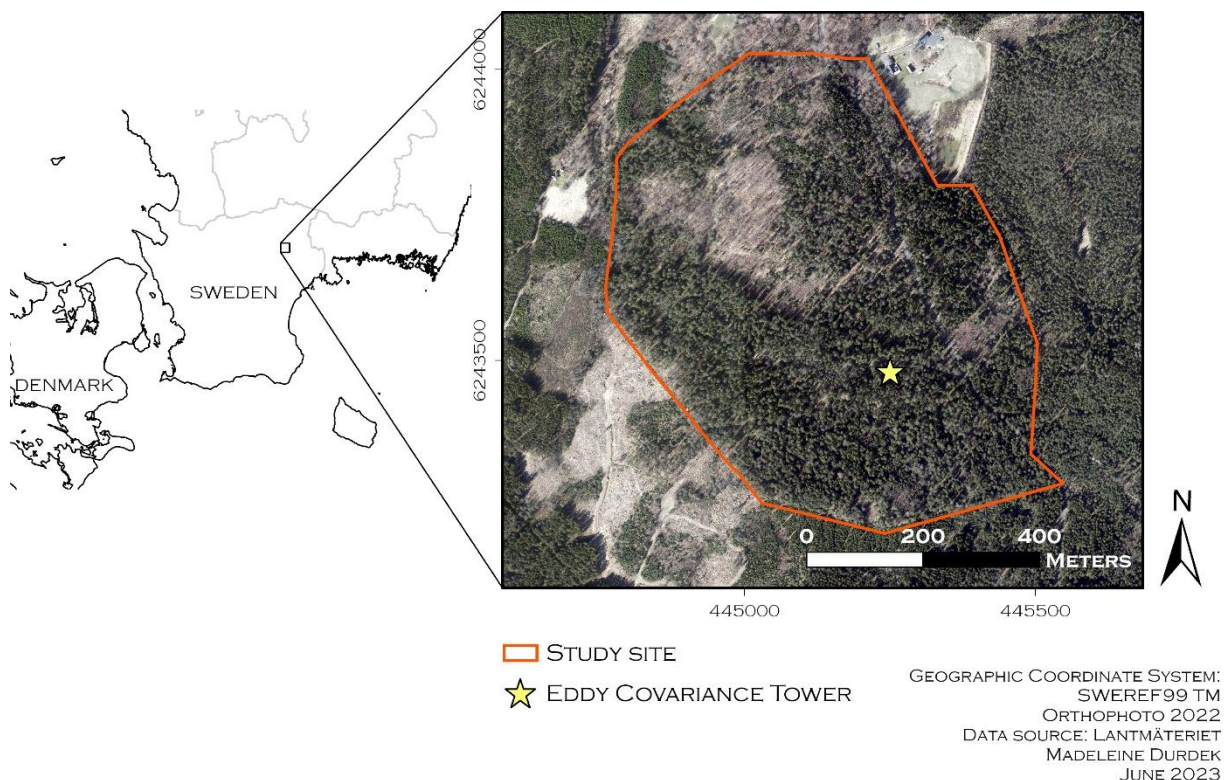
Figure 1. The Rumperöd forest and its Eddy Covariance tower situated in Skåne County in Southern Sweden

The Eddy Covariance (EC) tower was established in July 2013; however, because of thunderstorm damages in 2014, continuous readings for whole calendar years are available from 2015 (P. Vestin, personal communication, April 2023). The tower is 35 m tall and is equipped with a CPEC 200 flux system (Campbell Scientific, Inc, UT, USA) consisting of an ultrasonic anemometer (CSAT-3A, Campbell Scientific, Inc, UT, USA) and an infrared gas analyser (EC-

155, Campbell Scientific, Inc, UT, USA) for measurements of Carbon dioxide and water approximately 7 m above the forest canopy.

2.2   Methods overview

Forest inventories were conducted in 2014 and 2015 in 18 plots positioned on transects around the EC tower. Inventory data consists of tree species, tree height, and Diameter at Breast Height (DBH). Those attributes were used to quantify FSC. Three indices of FSC were calculated. First, the Gini index calculating variation in BA; second, the Rumperöd Index specifically created for this study that takes surface roughness and stand density into account; third, the β index reflecting the proportion of deciduous and coniferous trees. That third index was used to contrast between growing and dormant season. Flux data from 2015 to 2022 was sorted so that the strongest signal of VPD (yearly top 25%) was part of the analysis, which was a way to pre-select dry atmospheric conditions and remove the influence of precipitation on ET fluxes. Flux data was then sorted by wind direction to overlap flux data and FSC per transect.

2.3   Field measurements

Forest inventories were conducted in 2014 and 2015. Circular 200 m² plots were established along the North (N), South (S), West (W) and East (E) transects in 2014 and along the North-West (NW), North-East (NE), South-West (SW) and South-East (SE) transects in 2015 by Westin (2015). The plots were established at 50 m and 100 m away from the EC tower, apart from the NE transect where a plot had to be established 90 m from the tower, because of the presence of a road. Westin (2015) also established additional plots on the NW transect, situated at 200 and 325 m from the tower, to characterise the presence of a young birch stand (at 200 m) and one of a mature beech (at 325 m). Figure 2 displays the setup of the study. Individual plots are later referred to as the initial(s) of the cardinal direction followed by their distance from the tower. For instance, SE50 is the plot situated 50 m away from the tower in the SE direction. Plot data consists of tree height, DBH, tree species, health status, and centre plots' GPS coordinates. Data was provided by Patrik Vestin from the Department of Physical Geography and Ecosystem Science at Lund University.
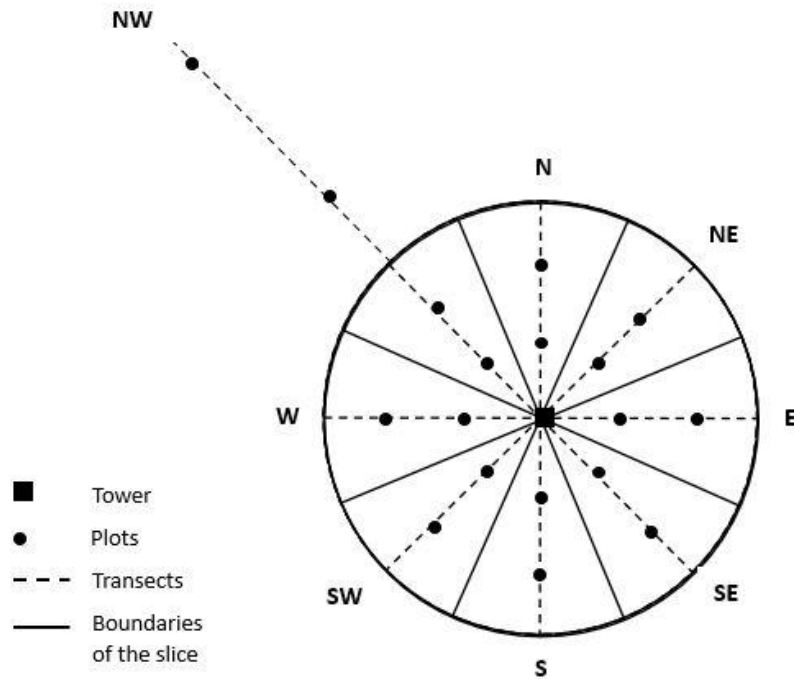
Figure 2. Schematic representation of the area and its division for the analysis. Note. This sketch aims at helping to visualise the setup of the study area but does not necessarily respect proportions.

The area around the EC tower was divided into 45° slices where each slice was assumed to be represented by the transect at its centre.

Tree height was measured using a Vertex IV hypsometer and a transponder T3 (Haglöf Sweden AB, Långsele, Sweden). The two instruments communicate by ultrasound. The transponder was fastened to every trunk at a height of 1.30 m. The Vertex was aimed at the transponder, then aimed at the treetop. Several readings of tree height were saved and an average calculated. DBH was cross-callipered at 1.30 m (Westin, 2015), because tree trunks are seldom completely round, and an average was calculated. Although this data was collected partly in 2014 and partly in 2015, it was assumed to be similar enough to be used together in the data analysis, for forests' growth is slow. Therefore, the small differences in tree height and DBH from one year to another would not have a big impact on FSC or fluxes. Trees of 2 m and higher were selected to be part of the analysis, regardless of their DBH. This decision was justified by the fact that the data was collected in a different way, where 2 m trees and higher were included in 2014, while Westin (2015) included trees from a height of 1.30 m.

A data overview of the ancillary measurements is shown in Table 1. The plots, for the most part dominated by spruce or birch, range from 8 to 57 measured trees, corresponding to the NW325 plot to the E50 plot, respectively.

Table 1. Overview of the field measurements data with tree species count, mean and standard deviation of basal area and height per plot.

Plot	Species (tree count)								Mean basal area (m²)	Mean height (m)
	Spruce	Pine	Oak	Beech	Birch	Alder	Rowan	**Total**		
N50	2				40			**42**	0.0003 ± 0.0002	2.6 ± 0.5
N100	21	1	1	1	2	3	2	**31**	0.01 ± 0.03	7.8 ± 8.1
NE50	14	2			3			**19**	0.04 ± 0.06	12.3 ± 9.1
NE90	8			1	23			**32**	0.01 ± 0.03	7.4 ± 5.5
E50	47		1	5	3		1	**57**	0.008 ± 0.02	7.4 ± 6.2
E100	24		7	2				**33**	0.02 ± 0.03	11.4 ± 9.4
SE50	14	3	3					**20**	0.04 ± 0.05	13.6 ± 7.7
SE100	27	1	5		11			**44**	0.01 ± 0.03	8.8 ± 6.0
S50	41		1					**42**	0.02 ± 0.02	13.6 ± 6.9
S100	9	1	1		12			**23**	0.03 ± 0.06	12.7 ± 8.7
SW50	29	1	1		7			**38**	0.02 ± 0.03	11.4 ± 6.6
SW100	8	1	2		13			**24**	0.02 ± 0.02	11.3 ± 5.1
W50	16		2		17			**35**	0.009 ± 0.006	9.8 ± 4.5
W100	19		5		2		1	**27**	0.02 ± 0.04	13.8 ± 6.8
NW50	20	1			6			**27**	0.02 ± 0.03	13.3 ± 8.0
NW100	16	1	4	3				**24**	0.01 ± 0.02	7.9 ± 5.9
NW200					18			**18**	0.001 ± 0.0002	5.5 ± 0.5
NW325				8				**8**	0.07 ± 0.06	21.1 ± 9.0

Note. Information in the present table is the one used for this study based on the tree selection described in section 2.3.

2.4   Forest Structural Complexity indices

FSC was first quantified per plot, before being averaged over all plots per transect. Three different approaches of FSC were tested. All approaches were meant to include few attributes and a simple mathematical system, as advised by McElhinny (2005). The first method used the Gini index to estimate the variation in BA. This index was previously used by Bourdier et al. (2016) to compute a light competition model. It was chosen for the present study both for its simplicity and to represent variation in BA instead of absolute stand BA. The Gini index ranges from 0 to 1, with 0 being no variation between the trees' BA, and 1 being a theoretical maximum variation of this attribute. Equation (1) was used to calculate it:

$$Gini = 2\frac{\sum_{i=1}^{n} i g_i}{nG} - \frac{n+1}{n} \tag{1}$$

Where g_i is the basal area of tree i in m², G the total basal area (m²) and n the number of trees. Note that tree i is based on the tree number sorted in ascending order.

Basal area BA, in m², was calculated for each individual tree using equation (2).

$$BA = \frac{\pi \cdot \left(\frac{DBH}{2}\right)^2}{10\,000} \tag{2}$$

6

Where DBH is the Diameter at Breast Height in cm, and 10 000 is used to scale BA to m².

The second approach is an attempt to include the influence of tree height and stand density, assumed to impact surface roughness and turbulence. Since EC data is used in this study, the necessity to account for surface roughness justifies this association of attributes. A higher canopy level increases surface roughness (Burba, 2021), which in turn decreases the footprint of fluxes. In other words, high surface roughness reduces the fetch of the contributing area. This index I created calculates the difference in tree height weighed by BA, for I assumed that tall trees with a small BA will have a reduced impact on turbulence compared to tall trees with a larger BA. Stand density was thereafter added to that calculation, similarly to Beckschäfer et al. (2013), where a value of 1 was added to the density to avoid giving too much weight to this parameter. This index thus primarily increases with the difference in tree height weighed by basal area and thereafter increases with increasing stand density. This index is referred to as the Rumperöd's Index (RI). Equation (3) was used to calculate it:

$$RI = \frac{\Sigma\,(\Delta h_i \cdot BA_i)}{\Sigma\,BA_i} \times (1 + \rho) \tag{3}$$

Where Δh_i is the difference between tree height h_i and the minimum tree height of the plot (in m). BA_i is the tree basal area in m², and ρ is the stand density expressed in number of trees per 10 m².

RI is a unitless measure of FSC that increases with difference in tree height, increased BA and density. However, because RI can differ greatly from one plot to another, making it difficult to appreciate the magnitude of FSC, RI values were normalised once all calculations were performed. Therefore, RI ranges from 0 to 1, with 1 being the most complex plot of the Rumperöd forest, based on equation (3).

The β index was used to estimate the influence of species composition. The proportion of coniferous trees was calculated and here again used as an index ranging from 0 to 1, where β = 0 represents 100% deciduous trees and β = 1 represents 100% coniferous trees.

Even if the selective felling of trees might have slightly modified biomass and species composition between 2015 and 2022, it was disregarded because of the assumed least impact on FSC and fluxes.

2.5 Eddy Covariance flux data

Measured EC flux data from 2015 to 2022 was analysed. It was directly provided by Patrik Vestin working at Lund University. Fluxes were derived from the method explained by Burba (2021) and calculated using EddyPro, version 7.0.7 (LI-COR Biosciences, NE, USA). Turbulent fluctuations of the raw EC data were extracted using half-hourly block-averaging. Fluxes were corrected for cross-wind for sonic temperature, double rotation for tilt correction, high-pass filtering (Moncrieff et al., 2005) and low-pass filtering (Horst, 1997). Fluxes were quality-controlled following the Mauder and Foken (2011) 0-1-2 system (quality flags ranging from 0 to 2, 0 being the best quality and 2 the worst). For the present analysis, quality flags of

0 only were retained. The flux data was also filtered based on friction velocity (u*) to avoid periods with low turbulence conditions and associated biases in flux estimates. Friction velocity below 0.3 m/s was therefore excluded from the analysis.

ET was calculated from the latent heat flux and VPD from air temperature and relative humidity. To maximise a range of values with significant turbulence, only daytime values were kept by excluding all data whose incoming shortwave radiation was below 20 W/m². This threshold, assumed to correspond to the transitional phase between night and daytime, has been widely used in EC gap-filling methods (Vekuri et al., 2023). To select the driest atmospheric conditions and remove the effect of precipitation on ET, only the top 25% of VPD were retained for the analysis. After comparing the sorted values with precipitation data from the closest meteorological station –Hästeveda, station no. 63160–, the great majority of the sorted values corresponded to 0 mm of precipitation. Precipitation data was retrieved from the Swedish Meteorological and Hydrological Institute (SMHI) (SMHI, n.d.-b). It motivated the choice of neglecting the outliers of precipitation and include all data from the flux sorting. The resulting filtered data was thereafter sorted by wind direction based on the 45° slices displayed in Figure 2. Table 2 gives details on the wind direction sorting.

Table 2. Azimuth values used to sort the flux data by wind direction.

Transect	Slice boundaries (°)	
N	> 337.5	22.5
NE	> 22.5	67.5
E	> 67.5	112.5
SE	> 112.5	157.5
S	> 157.5	202.5
SW	> 202.5	247.5
W	> 247.5	292.5
NW	> 292.5	337.5

To better understand the influence of species composition, ET was separately studied for the growing and the dormant season. The growing season was determined to be from April through October, according to data on vegetation period retrieved from SMHI (SMHI, n.d.-a).

2.6 Statistical analysis

The statistical analysis was performed to prove that the variation of ET in relation to VPD across transects is not due to random chance. A Generalised Linear Model (GLM) was used to test whether the residuals were dependent on transects or just on climatic variables, namely air temperature and net radiation. Soil water content was excluded because only two measuring probes are set up on the site and for a valid analysis it should be available for each transect, because soil moisture varies greatly spatially.

Since a GLM requires normally distributed data (Zuur et al., 2007), the residuals of ET to VPD (with ET as the dependent variable) for each year were tested for normality using IBM SPSS. It was done separately for the growing and the dormant season. It was however not tested

for the 2018-dormant season, as this dataset consisted of only 2 values. It resulted in 15 datasets. The built-in Kolmogorov-Smirnov and Shapiro-Wilk tests were used to assess of normality, with a p-value <0.05 implying that the data was not normally distributed. For cases with $n \geq 50$, the Kolmogorov-Smirnov p-value was chosen to determine normality, while the p-value from the Shapiro-Wilk test was chosen when $n <50$. Data transformations ($\log (x)$ and $\sqrt{x}$) were performed to attempt reaching normality if this was not the case.

The GLMs were performed in IBM SPSS using the built-in Wald Chi-Square and a 95% confidence interval. The null hypothesis was failed to be rejected, and significance accepted, if the p-value was below the threshold of 0.05. Two datasets (the 2019-dormant season and the 2018-growing season) were eventually tested, assuming that if significance was proved for them, dependence of ET on transects would be true for the rest of the datasets.

3   Results

3.1   Forest Structural Complexity

The analysis was performed using FSC indices per transect. Figure 3 shows these results, and results of FSC per plot are displayed in Appendix S1.
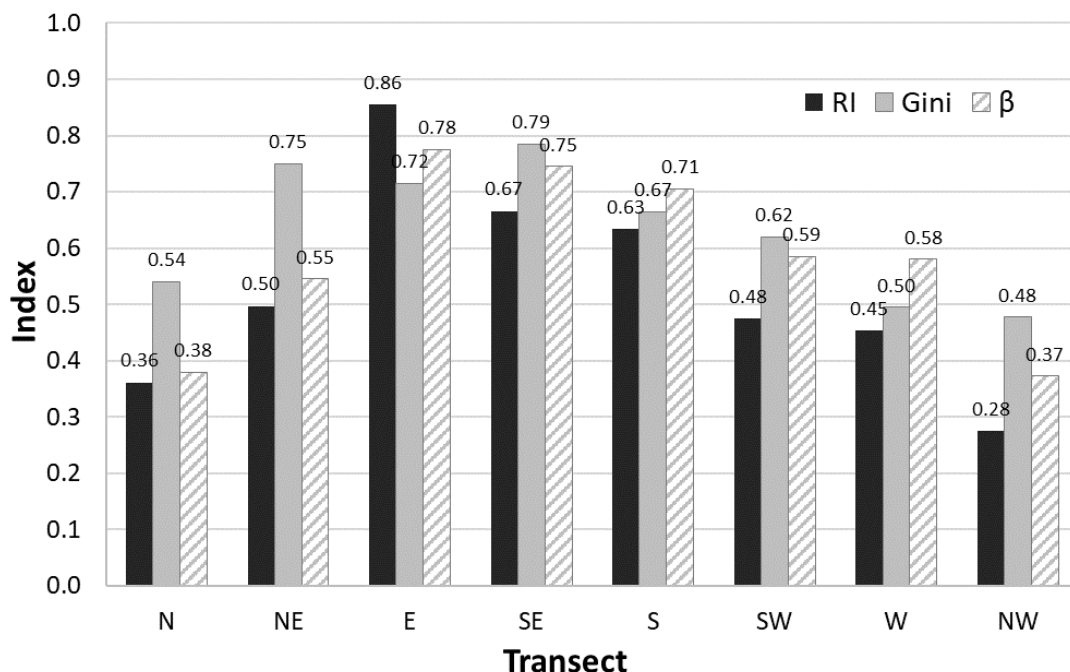
Figure 3. FSC per transect. A high RI corresponds to a high difference in tree height weighed by BA and a high stand density. A high Gini corresponds to a high variation in BA. β represents the proportion of conifers.

In Figure 3, β follows the pattern of Gini and RI overall. The E and SE transects present the most complexity, and the N and NW the least. The N and NW transects are mostly deciduous while the E, SE and S transects are >70% coniferous (see also Table 1).

In Appendix S1, a similar pattern among the indices is observed for the plots W50, W100, NW50, NW100, and NW200, but the rest of the plots show a greater variation in FSC depending on the index used. For instance, S50 has the lowest variation in BA, where Gini = 0.11.

However, RI = 0.75 in S50. It is also the plot with the highest proportion of coniferous trees (98%). Note that the Gini values are not necessarily below the RI values, i.e., complexity does not systematically increase when taking tree height and stand density into account. The maximum Gini of 0.82 is found in NE90, while the minimum Gini of 0.11 is found in S50. The maximum RI is found in E50, while the minimum RI of 0.04 is found in NW200, the young birch stand. The maximum β of 0.98 is found in S50, while the minimum β of 0 is found in NW200 and NW325.

3.2 Eddy Covariance measurements

3.2.1 VPD per transect

When looking at the yearly mean of VPD alone regardless of FSC indices (Figure 4), 2018 surpasses all other years, and this for every transect. The highest mean VPD was 1575 Pa for the SE transect in 2018, while the lowest was 624 Pa for the NE transect in 2015.
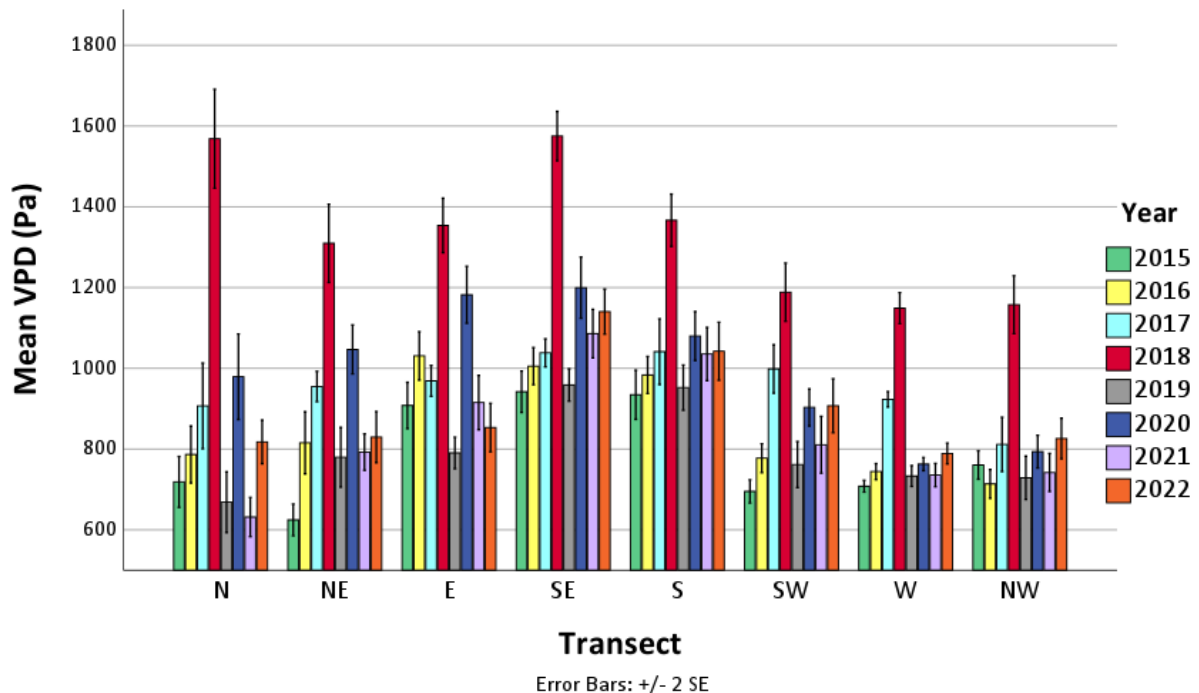
Figure 4. Annual mean VPD (in Pa) per transect for the years 2015-2022. The mean is that of the top 25% of VPD selected for each year. The error bars show the standard deviation of the distribution per transect and per year.

Mean VPD was globally higher for the E, S, and SE transects, and globally lower for the N and NE, and W, SW and NW transects (Figure 4). However, the 2018 mean VPD is the second highest for the N transect (VPD = 1569 Pa), which stands out compared to the other years in relation to the other transects. As VPD was the highest in 2018 and the lowest in 2015, these years are later compared in the response of ET to VPD in relation to FSC per transect (see Figure 8).

3.2.2 ET fluxes in relation to Forest Structural Complexity

The influence of FSC on ET fluxes is displayed in Figure 5 -Figure 7, which show the annual mean ET depending on Gini, RI and β, respectively. No clear trend is observed in the Gini index (Figure 5), but a decrease in ET is overall observed from Gini = 0.67 to Gini = 0.75. This negative relationship is however conflicted where the maximum Gini value (0.79) corresponds to some of the highest ET out of all years.
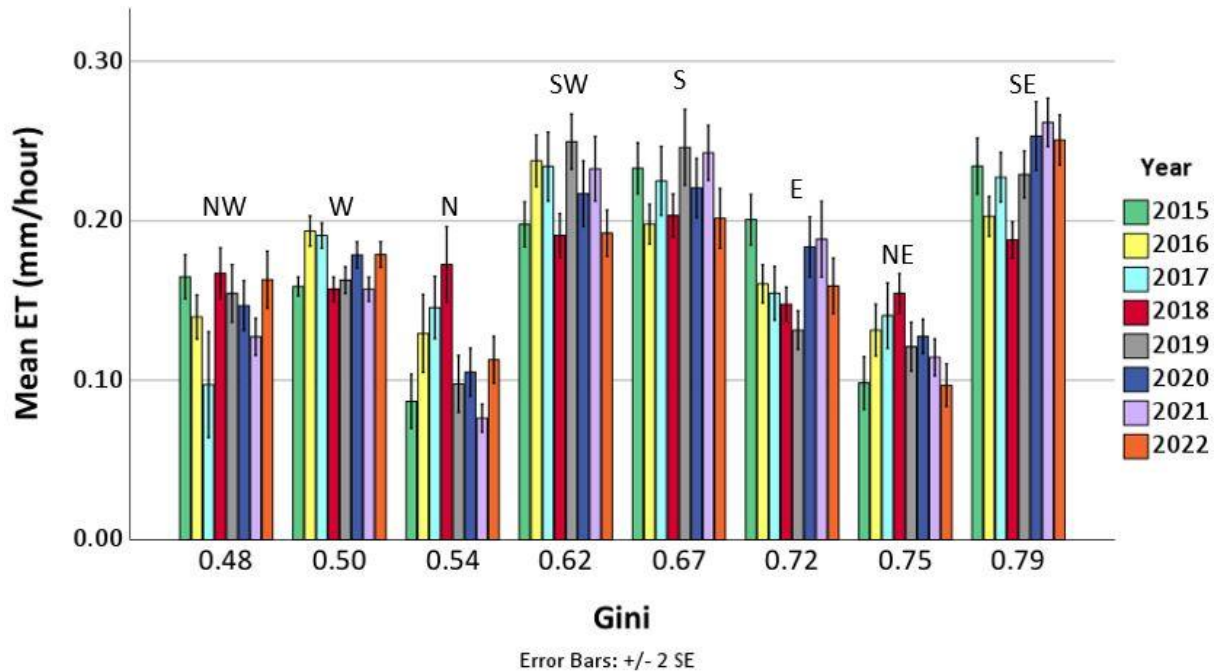
Figure 5. Annual mean ET depending on variation in BA (Gini index) for the years 2015-2022. The distribution of ET is based on selection of the top 25% of VPD selected each year. The error bars show the standard deviation of the distribution.

Overall, ET is the lowest in the N and NE transects where Gini = 0.54 and 0.75, respectively. It is overall the highest in the SW, S, and SE transects where Gini = 0.62, 0.67, and 0.79 respectively. ET is at its lowest (= 0.08 mm/hour) in 2021 for the N transect. It is at its highest (ET = 0.26 mm/hour) that same year where Gini = 0.79, corresponding to the SE transect.

FSC is represented by the RI in Figure 6. The only year for which the lowest ET corresponds to the highest RI value is 2018, with ET = 0.15 mm/hour for RI = 0.86, which corresponds to the E transect.
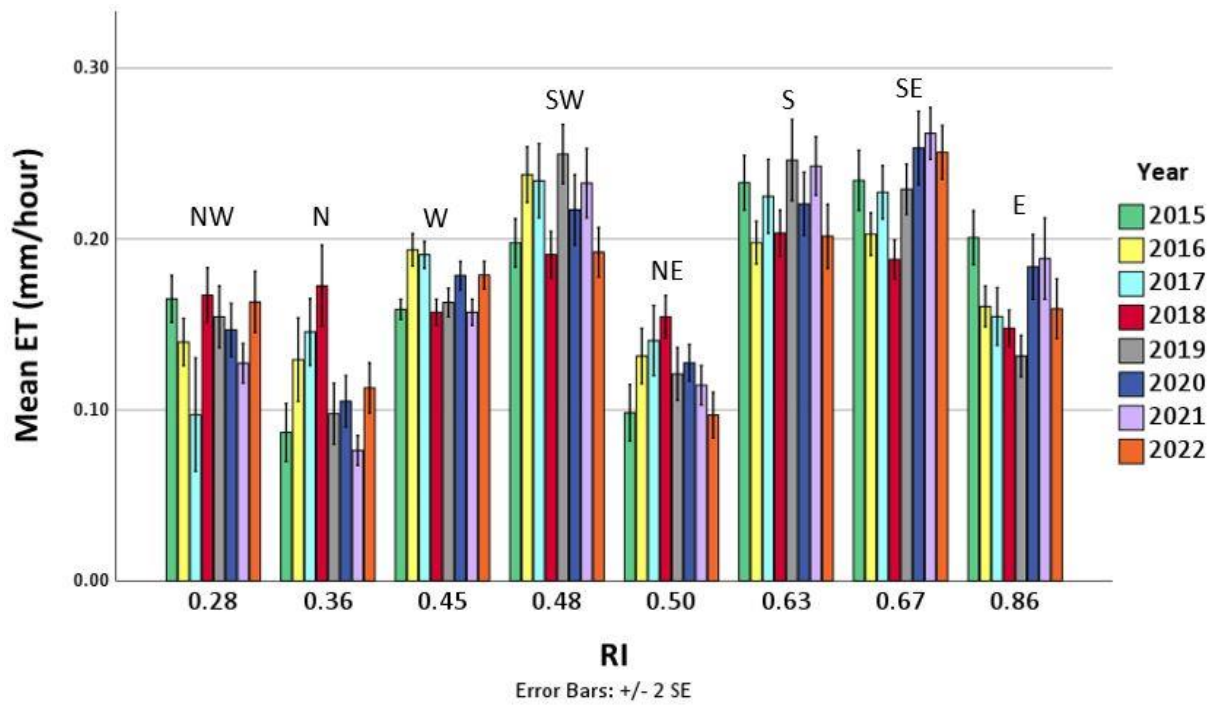
Figure 6. Annual mean ET depending on stand density and difference in tree height weighed by BA (RI) for the years 2015-2022. The distribution of ET is based on selection of the top 25% of VPD selected each year. The error bars show the standard deviation of the distribution.

No clear trend is observed among the other years, but ET is overall low at a low RI and high at a high RI. ET values are overall the lowest where RI = 0.36 and 0.50 (N and NE transect respectively), and the highest where RI = 0.63 and RI = 0.67 (S and SE transects respectively).

The annual mean ET is displayed against the β index in Figure 7. Apart from the highest value of β (= 0.78), corresponding to the E transect, a positive relationship is overall observed between ET and the proportion of coniferous trees.
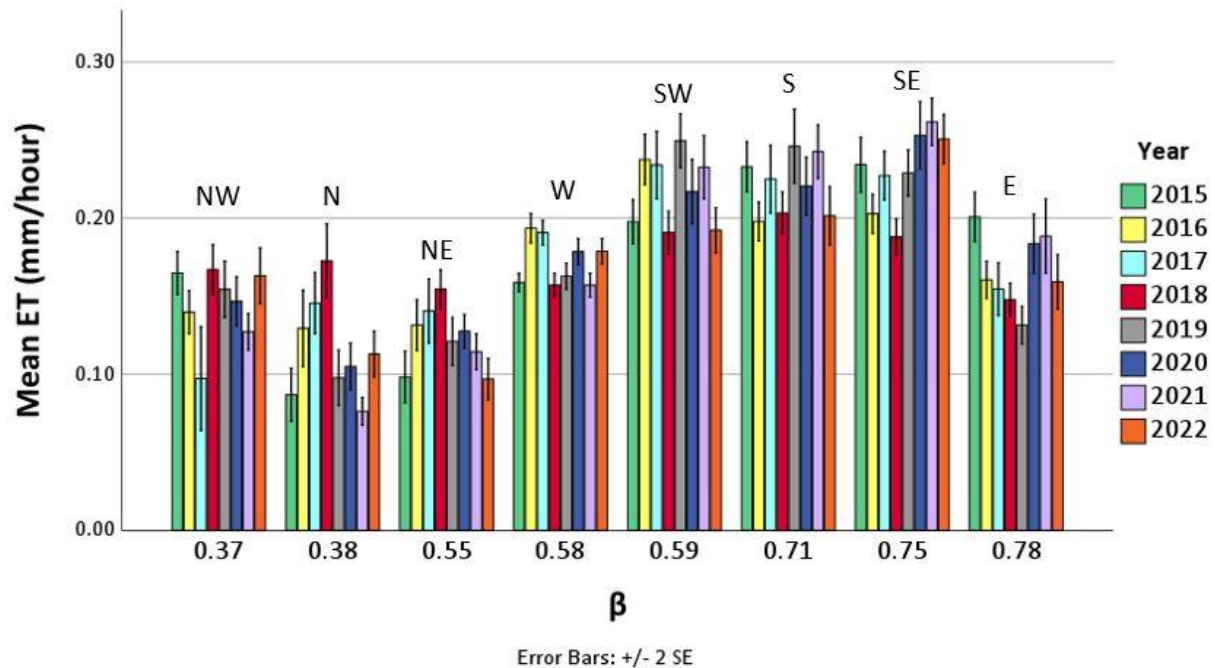
Figure 7. Annual mean ET depending on the proportion of coniferous species (β index) for the years 2015-2022. The distribution of ET is based on selection of the top 25% of VPD selected each year. The error bars show the standard deviation of the distribution.

ET is overall the lowest where $β = 0.37$, $β = 0.38$, and $β = 0.55$, that is, where the proportion of deciduous is close to or more than 50% of the stand. This corresponds to the NW, N, and NE transects respectively. In comparison, ET is overall the highest where $β = 0.59$, $β = 0.71$ and $β = 0.75$, which corresponds to the SW, S, and SE transect respectively.

The response of ET to FSC is summarised in *Table 3*.

Table 3. General overview of ET response to variation in FSC indices.

	RI		Gini		β	
	High	Low	High	Low	High	Low
High ET	S, SE		SW, S, SE		SW, S, SE	
Low ET	E	N, NE	NE	N	E	N, NW, NE

Overall, a high annual mean ET corresponds to a high FSC. Nevertheless, some exceptions are observed for the E and NE transects, and the lowest ET during the 2018 drought corresponds to the highest RI (E transect).

3.2.3 ET in relation to VPD

The annual mean VPD was overall the lowest in 2015, and the highest in 2018 (see Figure 4). The response of ET to VPD per transect was therefore compared between those years (Figure 8). ET is plotted against VPD for all years in Appendix S2 as scatter plots. To clearly visualise

the comparison between 2015 and 2018, trendlines were fitted on the residuals of the relationship displayed in S2. Polynomials of second order visually fitted the concave distribution of the residuals the best. This is an expected pattern that reflects the previously explained response of ET to increasingly dry conditions. In S2, the x-axis range is kept the same to compare the dispersion of the sorted VPD values. What it shows is that the top 25% of VPD can vary greatly from one year to another and across seasons.
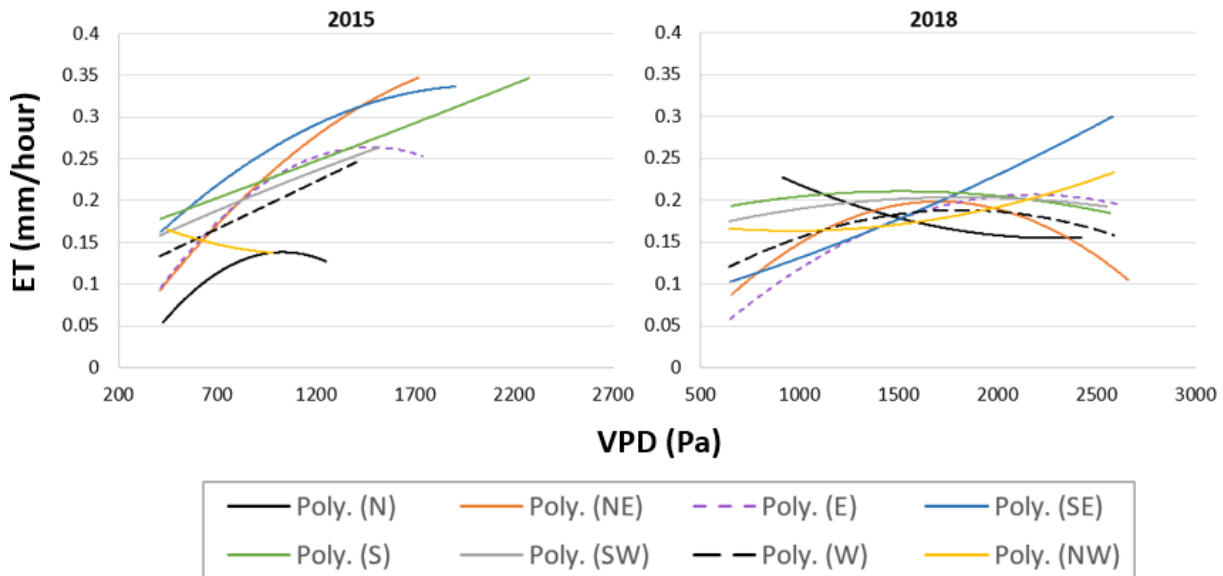

Figure 8. ET response to the top 25% of VPD in 2015 and 2018. Each curve represents a transect. Polynomials of second order ("Poly.") visually fitted the distribution of the residuals the best.

The previously explained non-linear, concave response of ET to increasing VPD, is more marked in 2018 than in 2015 (Figure 8). Values of ET in 2018 rarely exceeded 0.2 mm/hour when exposed to increasing VPD. The peak of the bell shape for the transects in 2018 occurs between VPD ≈ 1400 Pa and ≈ 2300 Pa. However, for that same year, the SE transect, and to a lower extent the NW transect, show a contrasting trend with a convex polynomial instead of concave. The N transect has its peak before all other transects, with ET ≈ 0.17 mm/hour at VPD ≈ 1400 Pa. The E transect has its peak where ET ≈ 0.2 mm/hour at VPD ≈ 2300 Pa. Note that the trend of the E transect shows lower ET than other transects from the start, i.e., where VPD ≈ 600 Pa.

In 2015, although polynomials were also fitted on the residuals, not all transects show that ET has been decreasing in response to increasing VPD. For instance, ET in the W, SW, S, SE, and NE transects keeps increasing, though with a weakening in the SE and NE transects at VPD ≈ 1500 Pa. The NW transect contrasts with the other relationships as the polynomial trend is convex and not concave. For both 2015 and 2018, a concave polynomial is fitted over the N transect residuals; however, in 2015, the N transect has its peak with ET ≈ 0.14 mm/hour at VPD ≈ 1100 Pa, while the peak of the bell in 2018 is observed at ET ≈ 0.17 mm/hour at VPD ≈ 1500 Pa in 2018.

The year 2021 was chosen to look at the distribution of residuals according to growing and dormant season (Figure 9) because it has a lot of residuals in both seasons (S2). The relationship between ET and VPD is compared between the most deciduous transect (NW) and the most coniferous one (E).
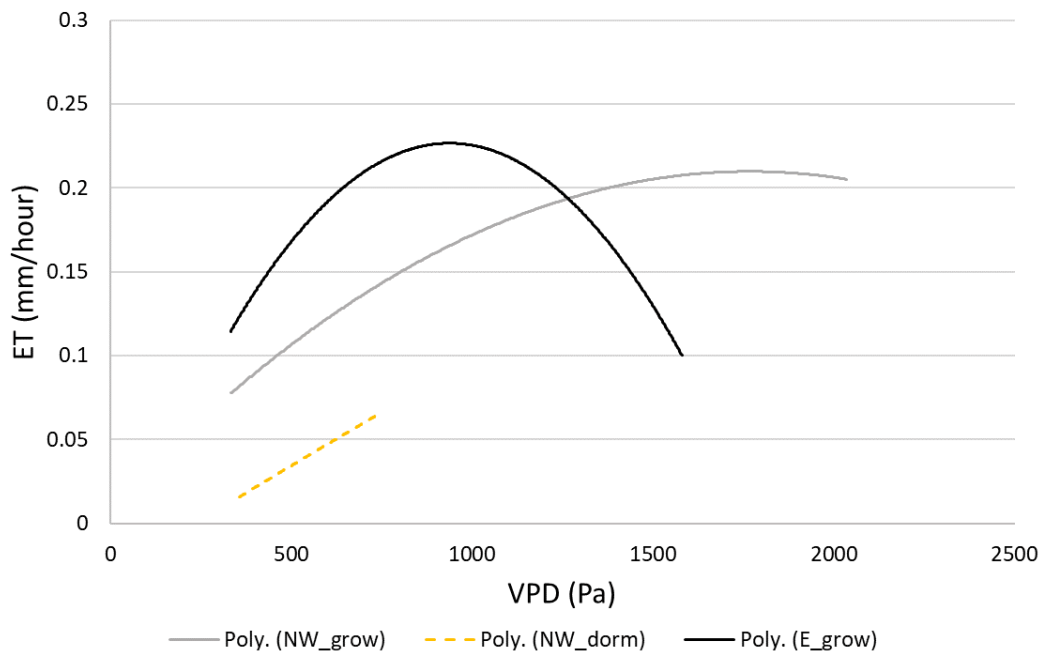
Figure 9. ET response to the top 25% of VPD in 2021 for the most coniferous (E) and the most deciduous transect (NW). The black curve represents the E transect during the growing season. The grey curve represents the NW transect during the growing season, and the yellow curve represents it during the dormant season. Polynomials of second order ("Poly.") visually fitted the distribution of the residuals the best.

The NW transect shows residuals in both seasons, while the E transect only has residuals in the growing season. The E transect shows a decrease of ET at lower VPD than the NW, i.e., the peak of ET ≈ 0.23 mm/hour at VPD ≈ 1000 Pa. The NW has its peak of ET has ≈ 0.21 mm/hour at VPD ≈ 1800 Pa. The dormant season, although not consisting of many residuals, shows no decrease in ET, and ET ranges between 0.01 and 0.06 mm/hour. Note that ET during the dormant season is mostly evaporation rather than ET since the trees have shed their leaves.

3.3   Statistical analysis

Results of the normality tests ran in IBM SPSS is shown in Appendix S3. The 2020-dormant season has a *n* number of residuals <50, with degrees of freedom *df* = 23. Its p-value from the Shapiro-Wilk test ("Sig." in S3) is 0.291, which indicates that those residuals are normally distributed. All other datasets have *df* >50, therefore the p-value of the Kolmogorov-Smirnov p-value indicates normality. The results show that the 2019-dormant season and the 2022-dormant season are normally distributed, for their p-value is 0.096 and 0.080 respectively; all other datasets are not.

Data transformations were possible for five of those non-normally distributed datasets, using the square root of x (i.e., the square root of ET plotted against the square root of VPD). The datasets concerned are the 2015, 2016 and 2017-dormant season, and the 2018 and 2022-growing season. The 2016-dormant season could also be transformed using $\log(x)$, which made it closer to normality than $\sqrt{x}$. S4 gives details on those datasets p-value after transformation.

Results from the GLM model are shown in Table 4 and Table 5 and show that air temperature was not significantly impacting the distribution of residuals in the 2019-dormant season (p-

value = 0.088). Apart from this case, all variables, including the fixed effect of the transect, have a significant influence on the residuals of ET to VPD, for the p-value is <0.05.

Table 4. Results from the GLM for the 2019-dormant season. The p-value is expressed as "Sig." and is significant for the transect and net radiation variables.

Source	Wald Chi-Square	Df	Sig.
Intercept	3.301	1	0.069
Transect	35.9	4	<0.001
Air temperature	2.9	1	0.088
Net radiation	128.7	1	<0.001

Dependent variable: Unstandardised Residuals

Only five transects are represented in the 2019-dormant season (Table 4), resulting in *df* = 4. For the 2018-growing season (Table 5), *df* = 7 meaning that all transects were represented in this dataset.

Table 5. Results from the GLM for the 2018-growing season using log (x). The p-value is expressed as "Sig." and is significant for the transect, air temperature, and net radiation variables.

Source	Wald Chi-Square	Df	Sig.
Intercept	25.1	1	<0.001
Transect	156.9	7	<0.001
Air temperature	16.4	1	<0.001
Net radiation	739.1	1	<0.001

Dependent variable: Unstandardised Residuals

Those results statistically show that the distribution of the residuals is not due to random chance. ET response to VPD is significantly dependent on the transects among other climatic variables. Moreover, the relationship is very strong since the p-value <0.001 for both datasets.

4 Discussion

A high variation in BA (Gini index) overall corresponds to high annual ET. Exceptions may be explained by species composition (β). I interpret high mean ET values as photosynthesis still taking place, thus corresponding to transects being less water-stressed than others. Deviations from this pattern may be attributable to species composition because they correspond to deciduous transects (Figure 5). A possible explanation resides in the physiological difference between coniferous and deciduous leaves. Leaf cuticular membranes are thicker and less permeable for conifers than they are for deciduous trees (Riederer & Schreiber, 2001). In other words, conifers retain water more than deciduous trees do. This could explain why, in Figure 8, the decrease of ET during the 2018 drought for the E transect occurred at higher VPD. Comparatively, ET in the N transect, mainly deciduous, is affected at lower VPD during the drought, and this was also the case in 2015 which was a milder year. Bachofen et al. (2023) found, using sap flow measurements, that absolute stand BA explained 30% of the total variance

of transpiration sensitivity to VPD. They also found that transpiration of deciduous species was higher than that of conifers. Even if our methods differ and the comparison is difficult, our results relate to each other in the sense that water fluxes are lower for conifers than for deciduous trees, and that a higher FSC contributes to maintaining water exchanges between the leaf and the atmosphere.

A high variation in tree height weighed by basal area and a high stand density (RI) overall corresponds to a high annual ET too. But contrary to the Gini index, the highest value of RI occurred at a lower mean ET, especially during the 2018 drought, for which ET was at its lowest (see Figure 6). What is worth noting here is that the highest RI corresponds to the E transect, and that the associated species composition and FSC does not follow the same assumption as for the Gini index. In other words, even if the transect is mainly coniferous and has a high FSC, it does not, in this case, result in high mean ET. An explanation for this likely resides in a difference in a limiting factor of ET. Distinction between evaporation and transpiration has been shown to mainly depend on stand density (Lundblad & Lindroth, 2002; Wedler et al., 1996). To quote Lundblad & Lindroth (2002), the "contribution of trees in a relatively closed forest under dry conditions can exceed 90% of total evapotranspiration, whereas in thinned or sparse stands, forest-floor evaporation may become the dominant component in total stand water flux". Therefore, in this case of a dense stand like the E transect and in the context of the dry conditions selected for this study, the low mean ET is attributable to low transpiration rather than to evaporation.

Lundblad & Lindroth (2002) also state that soil moisture is a limiting factor of transpiration, which brings forward that the E transect must experience depletion or scarcity in soil moisture. To understand why this is the case, I investigated the field measurements data (Table 1). it shows that the E transect is 78% composed of Norway spruce, a shallow-rooted species, and that it is the only coniferous species of the transect. As RI also accounts for surface roughness, the highest RI value corresponds to a rougher surface and the contributing area is likely close to the EC tower. It means that the E50 plot may contribute to the fluxes more than the E100 plot. Table 1 shows that E50 is denser and has more spruces than E100. Spruces, because of their shallow root architecture (Lundblad & Lindroth, 2002) compete for water in the topsoil layer, which is likely to be already depleted from water during dry periods. Lynch et al. (2012) explain that soil water content usually remains in deep soil layers under dry conditions. This is a situation where forest density associated with poor diversity increases competition between species (Kholdaenko et al., 2023). This may also explain why the E transect experienced a decrease in ET at lower VPD than the deciduous transect in 2021 (Figure 9).

The RI created for this study is simplistic and only includes three FSC attributes: tree height, BA and stand density. However, the distinction between the individual influence of surface roughness and stand density is not possible. From the field measurements data, stand density was indeed the highest for the E transect, and within it higher for the E50 plot than for the E100 plot. However, the sole surface roughness reflected in difference in tree height weighed by BA is undistinguishable in the RI. For future studies, I highly recommend quantifying FSC using only one attribute to better analyse the influence of the different forest properties, like it is the case with the Gini and the β index.

The higher stand density in the E transect enhancing competition between species relates to an important discussion point brought up by Bachofen et al. (2023): the influence of forest

management on water availability. Thinning practices increase water availability for the remaining trees, which in turns contributes to making them more vulnerable to droughts by increasing soil temperature and evaporation. Stand density is therefore an important attribute that may interfere and decrease ET fluxes, a problem accentuated by low species diversity.

Observed effects of canopy openness on evaporation fluxes are uncertain and hardly observable with the methods used here. The top 25% of VPD are more likely to occur during the growing season and the summer months, thus the datasets for the dormant season became very restricted for dry years. For instance, the severe drought that occurred in 2018 (Lindroth et al., 2020), shows only 2 values during the dormant season (S2). Other years, 2021 for example, show a larger proportion of readings during the dormant season. Hence, this sorting of the fluxes is more relevant to analyses of the growing season only. Nevertheless, when attempting to compare the dormant season for the most deciduous (NW) and the most coniferous (E) transect (Figure 9), the absence of residuals in the most coniferous transect is worth noting. In that same figure, ET decreases for the NW transect at higher VPD than the E transect. As previously mentioned, the E transect is a vulnerable, poorly diverse, and dense stand, which may justify the weaker resilience to increasing VPD in this case. Residuals being only present in the deciduous transect for the dormant season may imply that more evaporation could take place because radiation reaches the forest floor thanks to leaf phenology. Of course, there is a possibility that no wind was flowing from that direction under dry conditions in the dormant season, which marks the uncertainty of the interpretation.

The ET response to VPD is significantly dependent on transects. Even if this significance is attributable to variation in FSC, it should be kept in mind that soil moisture across the transects could also explain it, as it directly influences both evaporation and transpiration. Variation in soil moisture could also explain why VPD varies between transects (Figure 4), since a higher ET would contribute to making the above-canopy atmosphere moister and by that decrease VPD. But because soil moisture data is not available for each transect, it could not be included in the GLM. Furthermore, air moisture between transects could also be attributed to wind direction: the proximity of the Rumperöd forest with the Baltic Sea to the East could make easterly winds moister and thereby decrease VPD in the E transect. However, how much moisture would the ecosystems uptake between the sea and the forest is highly uncertain. Nevertheless, in regard of the rest of the results, the significant relationship between ET and VPD across transects suggests that FSC influences that relationship, regardless of the season. The dependence of the 2019-dormant season and the 2018-growing season was highly significant, which implies that the rest of the datasets are likely to be dependent on transects too. It is even more important that the significance is very high during the growing season of 2018 that experienced the meteorological drought. This supports the hypothesis that FSC influences water fluxes in the way that it helps trees maintain their hydraulic functioning under dry conditions. It is worth noting that, to this day, the influence of FSC on water fluxes has not been extensively studied. Studies on FSC and CCF have mainly been focused on their influence on biodiversity (Asbeck et al., 2023; Bartels & Macdonald, 2023).

This study analysed fluxes sorted by wind direction. In comparison, Leonard et al. (2022) used a model called flux footprint, which gives an accurate picture of the contributing area to the fluxes in percentages (Kljun et al., 2015). This method could improve the present study and investigate the influence of individual plots, as opposed to transects, which showed some

variation in surface roughness, species composition, and other complexity attributes. Furthermore, to analyse evaporation separately from transpiration fluxes would clarify the contribution to water losses from the forest. Lundblad & Lindroth (2002) explain that soil moisture is a limiting factor of ET. Continuous data on soil moisture per transect would be a way to critically look at ET and its spatial variability. Additionally, sap-flow measurement is a widely used method to estimate tree transpiration (Bachofen et al., 2023; Lagergren, 2001; Lundblad & Lindroth, 2002). Transpiration rates and response to VPD are species-specific (Chapin, 2003; Matheny et al., 2014). Thus, conducting sap-flow measurements per species and upscaling them to the plots based on plot data would improve our understanding of species diversity contribution to FSC and transpiration.

For instance, Lagergren (2001) investigated how thinning affects transpiration in a mixed pine and spruce forest, and found that spruce was much more affected than pine after a sudden increase in temperature. It raises the question of what other species would be more affected than others by droughts and climate change. A study by Song et al. (2022) brings forward that trees with long leaf lifespan –typically evergreen species– have a harder time recovering from droughts because of their reduced ability to replace drought-damaged tissues. Song et al. (2022) explain that leaf lifespan and leaf toughness are better predictors of drought recovery than hydraulic traits, making evergreen species more vulnerable to climate change. This contrasts with the previous explanation of the results in the way that conifers appeared to respond better to dry conditions. However, Song et al. (2022) mention "drought-damaged tissues", implying that evergreen trees would be more vulnerable to meteorological droughts. This paper investigates the years 2015 to 2022, and only 2018 was shown to have experienced a severe drought (Lindroth et al., 2020). For further investigations, an interesting input into FSC that would contribute to explaining the results is the influence of species diversity. A possible approach could quantify species evenness using the Pielou index (Pielou, 1966).

5   Conclusion and outlook

The Rumperöd forest structural complexity has an influence on ET fluxes that is observable using EC measurements. The relationship between ET and increasing FSC is overall clear, with a high annual mean ET corresponding to a high FSC. Variation in BA and difference in tree height weighed by BA illustrate this pattern. Species composition and stand density explain exceptions. A high mean ET is not to be interpreted as an increased ET, but rather that the water exchange from the leaf to the atmosphere could be maintained. On the contrary, less complex structures make the trees more vulnerable to dry atmospheric conditions, leading them to close their stomata and thereby impeding transpiration, which eventually leads to lower mean ET and decrease growth. This supports the hypothesis in the sense that complex structures help sustaining water exchanges under dry conditions. However, physiological differences between coniferous and deciduous trees explain that conifers can retain water easier than deciduous trees. Stand density creates competition, and if associated with poor species diversity, can lead a complex, coniferous stand to be more vulnerable to dry conditions. For future studies, I recommend using a flux footprint model that would specify the influence of individual plots. To clarify the contribution to water losses from the forest, I also suggest separating evaporation

from transpiration by using methods such as sap-flow measurements and by multiplying soil moisture probes on the site.

This study has several important implications. Firstly, it shows the importance of stand complexity and the role it plays in forests' response to dry atmospheric conditions. If less water is exchanged from the leaf to the atmosphere, positive feedbacks can result. It causes less precipitation and enhances water stress. Secondly, stomata opening intertwines the water and the carbon cycle: it is essential for water exchange, photosynthesis and carbon fixation to take place (Chapin et al., 2011a; Lambers et al., 2008). Carbon sequestration could be weakened by a lack of complexity in forest ecosystems, which makes FSC a relevant parameter to include in climate and carbon cycle models.

FSC positively influences biotope diversity (Asbeck et al., 2023). Considering the dramatic loss of biodiversity currently happening, and the time it takes to create or restore complexity in forests, the need to adapt forest management practices is urgent. This study shows another advantage of CCF for maintaining forests health and resilience in a changing climate.

6 References

Ahrens, C. D., & Henson, R. (2018). Atmospheric Humidity. In *Meteorology Today* (12th ed., pp. 91–113). Cengage.

Asbeck, T., Benneter, A., Huber, A., Margaritis, D., Buse, J., Popa, F., Pyttel, P., Förschler, M., Gärtner, S., & Bauhus, J. (2023). Enhancing structural complexity: An experiment conducted in the Black Forest National Park, Germany. *Ecology and Evolution*, *13*. https://doi.org/10.1002/ece3.9732

Bachofen, C., Poyatos, R., Flo, V., Martinez Vilalta, J., Mencuccini, M., Granda, V., & Grossiord, C. (2023). Stand structure of Central European forests matters more than climate for transpiration sensitivity to VPD. *Journal of Applied Ecology*. https://doi.org/10.1111/1365-2664.14383

Bartels, S. F., & Macdonald, S. E. (2023). Dynamics and recovery of forest understory biodiversity over 17 years following varying levels of retention harvesting. *Journal of Applied Ecology*, *n/a*(n/a). https://doi.org/10.1111/1365-2664.14366

Beckschäfer, P., Mundhenk, P., Kleinn, C., Ji, Y., Yu, D., & Harrison, R. (2013). Enhanced Structural Complexity Index: An Improved Index for Describing Forest Structural Complexity. *Open Journal of Forestry*, *3*, 23–29. https://doi.org/10.4236/ojf.2013.31005

Bednar-Friedl, B., Biesbroek, R., Schmidt, D. N., Alexander, P., Børsheim, K. Y., Carnicer, J., Georgopoulou, E., Haasnoot, M., Le Cozannet, G., Lionello, P., Lipka, O., Möllmann, C., Muccione, V., Mustonen, T., Piepenburg, D., & Whitmarsh, L. (2022). *Climate Change 2022: Impacts, Adaptation and Vulnerability. Contribution of Working Group II to the Sixth Assessment Report of the Intergovernmental Panel on Climate Change* (pp. 1817–1927).

Bettinger, P., Boston, K., Siry, J. P., & Grebner, D. L. (2017). Chapter 2—Valuing and Characterizing Forest Conditions. In P. Bettinger, K. Boston, J. P. Siry, & D. L. Grebner (Eds.), *Forest Management and Planning (Second Edition)* (pp. 21–63). Academic Press. https://doi.org/10.1016/B978-0-12-809476-1.00002-3

Bourdier, T., Cordonnier, T., Kunstler, G., Piedallu, C., Lagarrigues, G., & Courbaud, B. (2016). Tree Size Inequality Reduces Forest Productivity: An Analysis Combining Inventory Data for Ten European Species and a Light Competition Model. *PLoS ONE*, *11*(3), e0151852. https://doi.org/10.1371/journal.pone.0151852

Burba, G. (2021). *Eddy Covariance Method for Scientific, Regulatory, and Commercial Applications*. https://labinstruments.ru/upload/631b22e987ed5-LI-CORBook-EddyCovarianceMethodEdition22022_.pdf

Chapin, F. S., III. (2003). Effects of Plant Traits on Ecosystem and Regional Processes: A Conceptual Framework for Predicting the Consequences of Global Change. *Annals of Botany*, *91*(4), 455–463. https://doi.org/10.1093/aob/mcg041

Chapin, F. S., Matson, P. A., & Vitousek, P. M. (2011a). Carbon Inputs to Ecosystems. In F. S. Chapin, P. A. Matson, & P. M. Vitousek (Eds.), *Principles of Terrestrial Ecosystem Ecology* (pp. 123–156). Springer. https://doi.org/10.1007/978-1-4419-9504-9_5

Chapin, F. S., Matson, P. A., & Vitousek, P. M. (2011b). Water and Energy Balance. In F. S. Chapin, P. A. Matson, & P. M. Vitousek (Eds.), *Principles of Terrestrial Ecosystem Ecology* (pp. 93–122). Springer. https://doi.org/10.1007/978-1-4419-9504-9_4

Chen, H. (n.d.). *Köppen climate classification*. Hans Chen. Retrieved 10 April 2023, from http://hanschen.org/koppen

Delin, E. (2019). *Forest Reaction to the 2018 Drought: Comparing the Hyltemossa and Rumperöd Forests* [Bachelor Thesis, Lund University]. http://lup.lub.lu.se/student-papers/record/8987829

Ekholm, A., Lundqvist, L., Petter Axelsson, E., Egnell, G., Hjältén, J., Lundmark, T., & Sjögren, J. (2023). Long-term yield and biodiversity in stands managed with the selection system and the rotation forestry system: A qualitative review. *Forest Ecology and Management*, *537*, 120920. https://doi.org/10.1016/j.foreco.2023.120920

Gamelin, B. L., Feinstein, J., Wang, J., Bessac, J., Yan, E., & Kotamarthi, V. R. (2022). Projected U.S. drought extremes through the twenty-first century with vapor pressure deficit. *Scientific Reports*, *12*(1), Article 1. https://doi.org/10.1038/s41598-022-12516-7

Grossiord, C., Buckley, T. N., Cernusak, L. A., Novick, K. A., Poulter, B., Siegwolf, R. T. W., Sperry, J. S., & McDowell, N. G. (2020). Plant responses to rising vapor pressure deficit. *New Phytologist*, *226*(6), 1550–1566. https://doi.org/10.1111/nph.16485

Gundersen, P., Schmidt, I., & Raulund-Rasmussen, K. (2011). Leaching of nitrate from temperate forests—Effects of air pollution and forest management. *Environmental Reviews*, *14*, 1–57. https://doi.org/10.1139/a05-015

Horst, T. W. (1997). A SIMPLE FORMULA FOR ATTENUATION OF EDDY FLUXES MEASURED WITH FIRST-ORDER-RESPONSE SCALAR SENSORS. *Boundary-Layer Meteorology*, *82*(2), 219–233. https://doi.org/10.1023/A:1000229130034

Johnson, J., & Ferrell, W. (2006). Stomatal Response to Vapour Pressure Deficit and the Effect of Plant Water Stress. *Plant, Cell & Environment*, *6*, 451–456. https://doi.org/10.1111/1365-3040.ep11588103

Kholdaenko, Y. A., Babushkina, E. A., Belokopytova, L. V., Zhirnova, D. F., Koshurnikova, N. N., Yang, B., & Vaganov, E. A. (2023). The More the Merrier or the Fewer the Better Fare? Effects of Stand Density on Tree Growth and Climatic Response in a Scots Pine Plantation. *Forests*, *14*(5), 915. https://doi.org/10.3390/f14050915

Kljun, N., Calanca, P., Rotach, M. W., & Schmid, H. P. (2015). A simple two-dimensional parameterisation for Flux Footprint Prediction (FFP). *Geoscientific Model Development*, *8*(11), 3695–3713. https://doi.org/10.5194/gmd-8-3695-2015

Lagergren, F. (2001). *Effects of Thinning, Weather and Soil Moisture on Tree and Stand Transpiration in a Swedish Forest*.

Lambers, H., Chapin, F. S., & Pons, T. L. (2008). Photosynthesis. In H. Lambers, F. S. Chapin, & T. L. Pons (Eds.), *Plant Physiological Ecology* (pp. 11–99). Springer. https://doi.org/10.1007/978-0-387-78341-3_2

Leonard, R., Moore, P., Krause, S., Chasmer, L., Devito, K., Petrone, R., Mendoza, C., Waddington, J., & Kettridge, N. (2022). Forest Stand Complexity Controls Ecosystem-Scale Evapotranspiration Dynamics: Implications for Landscape Flux Simulations. *Hydrological Processes*, *36*. https://doi.org/10.1002/hyp.14761

Lindroth, A., Holst, J., Linderson, M.-L., Aurela, M., Biermann, T., Heliasz, M., Chi, J., Ibrom, A., Kolari, P., Klemedtsson, L., Krasnova, A., Laurila, T., Lehner, I., Lohila, A., Mammarella, I., Mölder, M., Löfvenius, M. O., Peichl, M., Pilegaard, K., … Nilsson, M. (2020). Effects of drought and meteorological forcing on carbon and water fluxes in Nordic forests during the dry summer of 2018. *Philosophical Transactions of the Royal Society B: Biological Sciences*, *375*(1810), 20190516. https://doi.org/10.1098/rstb.2019.0516

Lundblad, M., & Lindroth, A. (2002). Stand transpiration and sapflow density in relation to weather, soil moisture and stand characteristics. *Basic and Applied Ecology*, *3*(3), 229–243. https://doi.org/10.1078/1439-1791-00099

Lundmark, H., Josefsson, T., & Östlund, L. (2013). The history of clear-cutting in northern Sweden – Driving forces and myths in boreal silviculture. *Forest Ecology and Management*, *307*, 112–122. https://doi.org/10.1016/j.foreco.2013.07.003

Lynch, J., Marschner, P., & Rengel, Z. (2012). Chapter 13—Effect of Internal and External Factors on Root Growth and Development. In P. Marschner (Ed.), *Marschner's Mineral Nutrition of Higher Plants (Third Edition)* (pp. 331–346). Academic Press. https://doi.org/10.1016/B978-0-12-384905-2.00013-3

Macpherson, M. F., Kleczkowski, A., Healey, J. R., Quine, C. P., & Hanley, N. (2017). The effects of invasive pests and pathogens on strategies for forest diversification. *Ecological Modelling*, *350*, 87–99. https://doi.org/10.1016/j.ecolmodel.2017.02.003

Matheny, A. M., Bohrer, G., Vogel, C. S., Morin, T. H., He, L., Frasson, R. P. de M., Mirfenderesgi, G., Schäfer, K. V. R., Gough, C. M., Ivanov, V. Y., & Curtis, P. S. (2014). Species-specific transpiration responses to intermediate disturbance in a northern hardwood forest. *Journal of Geophysical Research: Biogeosciences*, *119*(12), 2292–2311. https://doi.org/10.1002/2014JG002804

Mauder, M., & Foken, T. (2011). Documentation and Instruction Manual of the Eddy Covariance Software Package TK2. *Arbeitsergebnisse, Universität Bayreuth, Abteilung Mikrometeorologie, ISSN 1614-8916*, *46*. https://doi.org/10.5194/bg-5-451-2008

McElhinny, C., Gibbons, P., Brack, C., & Bauhus, J. (2005). Forest and woodland stand structural complexity: Its definition and measurement. *Forest Ecology and Management*, *218*(1–3), 1–24. https://doi.org/10.1016/j.foreco.2005.08.034

Moncrieff, J., Clement, R., Finnigan, J., & Meyers, T. (2005). Averaging, Detrending, and Filtering of Eddy Covariance Time Series. In X. Lee, W. Massman, & B. Law (Eds.), *Handbook of Micrometeorology: A Guide for Surface Flux Measurement and Analysis* (pp. 7–31). Springer Netherlands. https://doi.org/10.1007/1-4020-2265-4_2

Paul-Limoges, E., Wolf, S., Eugster, W., Hörtnagl, L., & Buchmann, N. (2017). Below-canopy contributions to ecosystem CO 2 fluxes in a temperate mixed forest in Switzerland. *Agricultural and Forest Meteorology*, *247*, 582–596. https://doi.org/10.1016/j.agrformet.2017.08.011

Pielou, E. C. (1966). The measurement of diversity in different types of biological collections. *Journal of Theoretical Biology*, *13*, 131–144. https://doi.org/10.1016/0022-5193(66)90013-0

Riederer, M., & Schreiber, L. (2001). Protecting against water loss: Analysis of the barrier properties of plant cuticles. *Journal of Experimental Botany*, *52*(363), 2023–2032. https://doi.org/10.1093/jexbot/52.363.2023

Saarsalmi, A., Tamminen, P., Kukkola, M., & Hautajarvi, R. (2010). Whole-tree harvesting at clear-felling: Impact on soil chemistry, needle nutrient concentrations and growth of Scots pine. *Scandinavian Journal of Forest Research - SCAND J FOREST RES*, *25*, 148–156. https://doi.org/10.1080/02827581003667314

Seppälä, M. (Ed.). (2005). *The physical geography of Fennoscandia*. Oxford University Press.

SMHI. (n.d.-a). *Klimatindikator—Vegetationsperiodens längd | SMHI*. Retrieved 20 April 2023, from https://www.smhi.se/klimat/klimatet-da-och-nu/klimatindikatorer/klimatindikator-vegetationsperiodens-langd-1.7887

SMHI. (n.d.-b). *Nederbörd | SMHI*. Retrieved 19 April 2023, from https://www.smhi.se/data/meteorologi/nederbord

Song, Y., Sterck, F., Zhou, X., Liu, Q., Kruijt, B., & Poorter, L. (2022). Drought resilience of conifer species is driven by leaf lifespan but not by hydraulic traits. *The New Phytologist*, *235*(3), 978–992. https://doi.org/10.1111/nph.18177

Spiecker, H. (2003). Silvicultural management in maintaining biodiversity and resistance of forests in Europe—Temperate zone. *Journal of Environmental Management*, *67*(1), 55–65. https://doi.org/10.1016/S0301-4797(02)00188-3

Vekuri, H., Tuovinen, J.-P., Kulmala, L., Papale, D., Kolari, P., Aurela, M., Laurila, T., Liski, J., & Lohila, A. (2023). A widely-used eddy covariance gap-filling method creates systematic bias in carbon balance estimates. *Scientific Reports*, *13*(1), Article 1. https://doi.org/10.1038/s41598-023-28827-2

Vestin, P. (2017). *Effects of forest management on greenhouse gas fluxes in a boreal forest*.

Vestin, P., Mölder, M., Kljun, N., Cai, Z., Hasan, A., Holst, J., Klemedtsson, L., & Lindroth, A. (2020). Impacts of Clear-Cutting of a Boreal Forest on Carbon Dioxide, Methane and Nitrous Oxide Fluxes. *Forests*, *11*(9), Article 9. https://doi.org/10.3390/f11090961

Vestin, P., Mölder, M., Kljun, N., Cai, Z., Hasan, A., Holst, J., Klemedtsson, L., & Lindroth, A. (2022). Impacts of stump harvesting on carbon dioxide, methane and nitrous oxide fluxes. *IForest - Biogeosciences and Forestry*, *15*, 148–162. https://doi.org/10.3832/ifor4086-015

Vitousek, P. M., Gosz, J. R., Grier, C. C., Melillo, J. M., Reiners, W. A., & Todd, R. L. (1979). Nitrate losses from disturbed ecosystems. *Science (New York, N.Y.)*, *204*(4392), 469–474. https://doi.org/10.1126/science.204.4392.469

Wedler, M., Heindl, B., Hahn, S., Köstner, B., Bernhofer, Ch., & Tenhunen, J. D. (1996). Model-based estimates of water loss from "patches" of the understory mosaic of the Hartheim Scots pine plantation. *Theoretical and Applied Climatology*, *53*(1), 135–144. https://doi.org/10.1007/BF00866418

Westin, J. (2015). *Quantification of a continuous-cover forest in Sweden using remote sensing techniques* [Master Thesis, Lund University]. http://lup.lub.lu.se/student-papers/record/8561391

Zhang, D., Du, Q., Zhang, Z., Jiao, X., Song, X., & Li, J. (2017). Vapour pressure deficit control in relation to water transport and water productivity in greenhouse tomato

production during summer. *Scientific Reports*, *7*(1), Article 1.
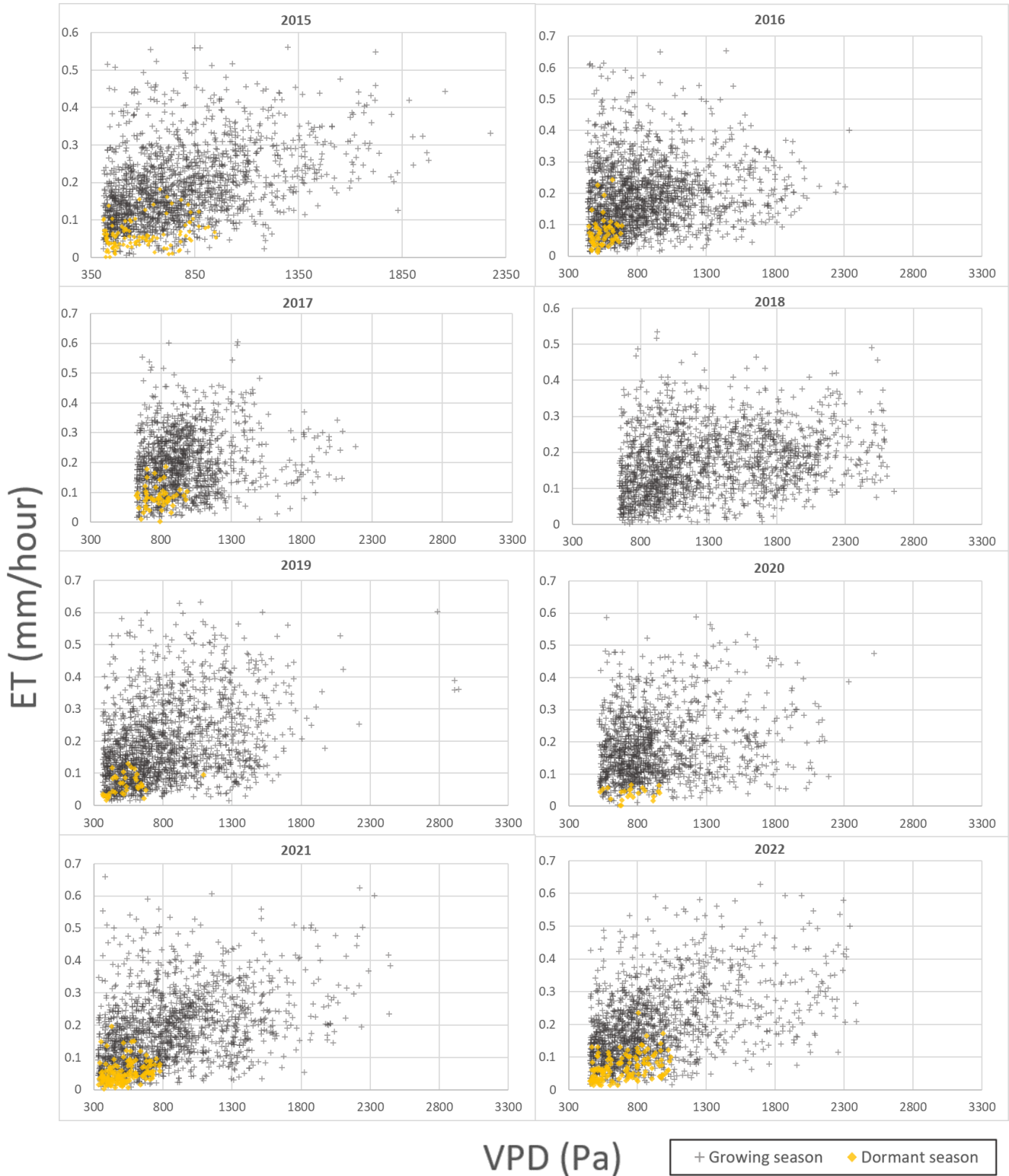https://doi.org/10.1038/srep43461

Zuur, A. F., Ieno, E. N., & Smith, G. M. (2007). *Analysing ecological data*. Springer.

7 Appendix
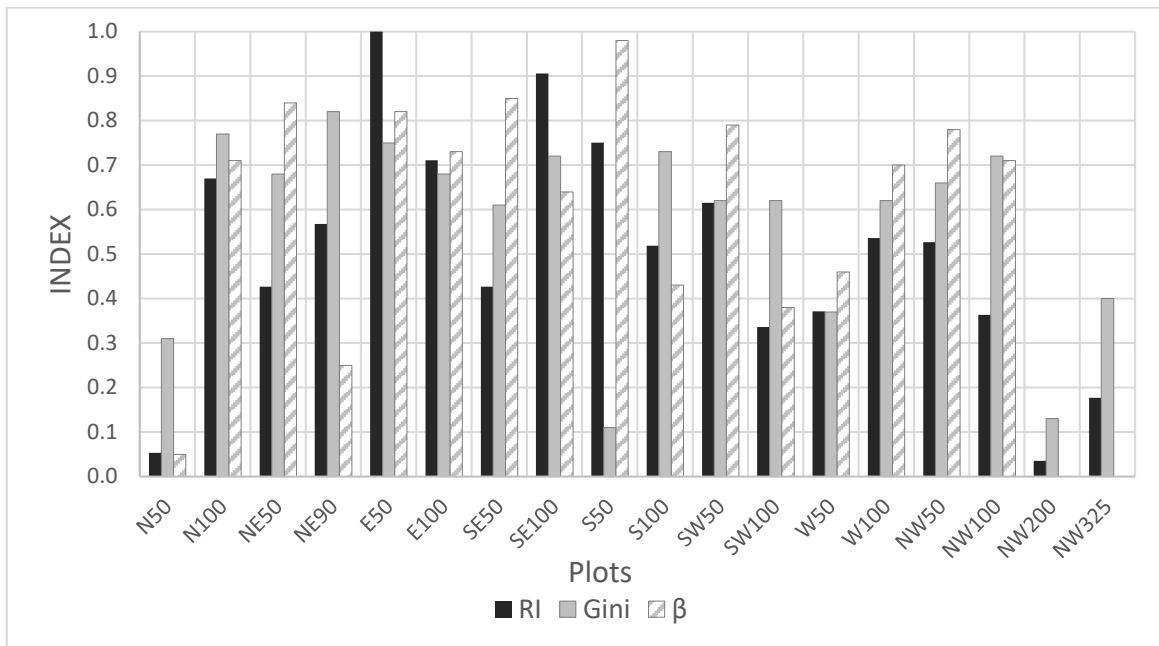
S1. All three indices per plot, showing the variation that can occur within a transect.

S2. ET response to VPD (top 25%) from 2015 to 2022 in the Rumperöd forest (all transects).

S3. Tests of Normality performed in IBM SPSS with p-values of the residuals for all years; res_grow and res_dorm designate the residuals of the growing and the dormant season, respectively.

	Kolmogorov-Smirnov[a]			Shapiro-Wilk		
	Statistic	Df	Sig.	Statistic	Df	Sig.
2015_res_grow	0.071	1676	<0.001	0.949	1676	<0.001
2015_res_dorm	0.120	112	<0.001	0.941	112	<0.001
2016_res_grow	0.073	1709	<0.001	0.936	1709	<0.001
2016_res_dorm	0.159	56	0.001	0.826	56	<0.001
2017_res_grow	0.043	1218	<0.001	0.975	1218	<0.001
2017_res_dorm	0.132	51	0.026	0.946	51	0.022
2018_res_grow	0.053	1678	<0.001	0.973	1678	<0.001
2019_res_grow	0.085	1732	<0.001	0.941	1732	<0.001
2019_res_dorm	0.067	151	0.096	0.972	151	0.003
2020_res_grow	0.072	1256	<0.001	0.950	1256	<0.001
2020_res_dorm	0.112	23	0.200*	0.950	23	0.291
2021_res_grow	0.064	1527	<0.001	0.948	1527	<0.001
2021_res_dorm	0.144	142	<0.001	0.861	142	<0.001
2022_res_grow	0.068	1424	<0.001	0.967	1424	<0.001
2022_res_dorm	0.073	134	0.080	0.947	134	<0.001

*. This is a lower bound of the true significance.

[a]. Lillefors Signficance Correction

S4. P-values reached after data transformations using log (x) or √x.

Dataset	$\log (x)$	$\sqrt{x}$
2015_dorm	<0.001	0.200
2016_dorm	0.200	0.181
2017_dorm	<0.001	0.075
2018_grow	<0.001	0.200
2022_grow	<0.001	0.145